# Compressive Sampling based Multiple Symbol Differential Detection for UWB IR Signals

Shahzad Gishkori*, Geert Leus*, Vincenzo Lottici†
* Faculty of EEMCS, Delft University of Technology, Delft, The Netherlands
† Deptt. of Information Engineering, University of Pisa, Pisa, Italy
Emails: s.s.gishkori@tudelft.nl; g.j.t.leus@tudelft.nl; vincenzo.lottici@iet.unipi.it

***Abstract*—In this paper, a compressive sampling (CS) based multiple symbol differential detector is proposed, using the principle of a generalized likelihood ratio test (GLRT). The proposed detector works on the compressed samples directly, thereby avoiding the reconstruction step and thus resulting in a reduced implementation complexity along with a reduced sampling rate (much below the Nyquist rate). We also propose the compressed sphere decoder (CSD) to resolve the detection of multiple symbols. Our proposed detector is valid for scenarios where the measurement matrices are the same as well as where they are different for each received symbol.**

***Index Terms*—compressive sampling, multiple symbol differential detection, ultra-wideband**

## I. Introduction

Equipped with the prospects of high data rates, fine timing resolution and multipath immunity, the impulse radio ultra wideband (IR-UWB) technology has potentially made its way to the forefront of short range communications, in recent times [1], [2]. Owing to the large bandwidth, the received signal consists of hundreds of separable copies of the transmitted pulse [3]. Exploiting this rich multipath environment can lead to a better performance of the system. The optimum strategies employ Rake receivers to collect most of the received energy but are bottle-necked by the number of rake fingers (that grow proportional to the number of propagation paths) and accurate channel estimation, which result in increased computational complexity along with high power consumption [4], [5]. New techniques are needed to remove these impediments in order to make UWB systems a commercial success.

A number of autocorrelation receivers (AcRs) based suboptimal (noncoherent) techniques have been proposed in the literature to circumvent the constraint of channel estimation, e.g., the transmitted reference (TR) and the differential detection (DD) schemes [6], [7], [8]. In TR, each transmitted information pulse is accompanied by an unmodulated pulse as a reference. The receiver then correlates the reference pulse with the modulated pulse to decipher the information symbol. In contrast to TR, the DD scheme employs differential encoding of the information symbols and thereby avoids transmission of a reference pulse. The information is decoded by correlating the successively received pulses. The performance of the DD scheme can be improved by using multiple symbol differential detection (MSDD) [9], [10], [11]. In MSDD, the correlation operation is not restricted to consecutive symbols only but involves a block of received symbols which leads to the detection of a block of information symbols simultaneously and thus results in an enhanced performance. Despite the benefits offered by the aforementioned techniques, the correlation operation involved incurs additional challenges, i.e., if carried out in the analog domain, it can cause long delays and if carried out in the digital domain, it necessitates Nyquist rate sampling of the received signal. It is hard to implement delay lines in the analog domain and the Nyquist rate sampling can heavily stress the analog-to-digital converters (ADCs) causing high power consumption in the digital domain.

With respect to the digital implementation of the correlation based receivers, compressive sampling (CS) has recently been proposed in literature as a technique which reduces the sampling rate much below the Nyquist rate [12], [13]. In this technique, the received signal is converted to compressed samples by taking a limited number of snapshots or measurements in the analog domain [14], [15]. Each measurement represents a compressed sample. The measurement process can be thought of as a matrix multiplication of linear functionals. The received signal is reconstructed from its compressed samples by a reconstruction process governed by one of the available reconstruction algorithms, which is then followed by the detection process. CS has been used in connection with UWB in [16] for coherent receivers and in [17] for the joint time of arrival estimation and data decoding. In [18] we proposed noncoherent differential detectors based on CS. Apart from proposing joint reconstruction and detection methods, we also proposed a detector based on compressed samples, labeled as the direct compressed differential detector (DC-DD). The DC-DD skips the reconstruction step and thus can reduce the implementation complexity of the compressed differential detector. This idea was extended to decision feedback differential detection (DF-DD) in [19]. The implementation of DC-DD is still limited by the fact that the measurement process is the same for each symbol.

In this paper we propose a compressive sampling based MSDD (CMSDD) that works on the principle of a generalized likelihood ratio test (GLRT) [20]. The performance of the detector is increased by employing multiple symbols but at the same time the implementation complexity is reduced by skipping the reconstruction step. We also propose a compressed

This work is supported in part by NWO-STW under the VICI program (project 10382).

sphere decoder to reduce the decoding complexity of the block of symbols.

*Notations*: Matrices are in upper case bold while column vectors are in lower case bold, $[\mathbf{a}]_i$ is the $i$th entry of the vector $\mathbf{a}$, $\hat{\mathbf{a}}$ is the estimate of $\mathbf{a}$, $\mathbf{I}_N$ is the identity matrix of size $N \times N$, $(\cdot)^T$ is transpose, $(\cdot)^\dagger$ is pseudo-inverse, $\otimes$ stands for the Kronecker product, $\perp$ depicts orthogonality, diag$\{\cdot\}$ presents a block diagonal matrix having the arguments along its main diagonal and $\triangleq$ defines an entity.

## II. Signal Model

In the present IR-UWB signal model, we assume that each symbol is conveyed by a pulse $q(t)$ of duration $T_q$ much less than the symbol interval $T_s$, i.e., $T_q \ll T_s$. The transmitted signal is composed of a block of $Q+1$ symbols, i.e.,

$$s(t) = \sum_{k=0}^{Q} b_k q(t - kT_s) \tag{1}$$

where $b_k \in \{\pm 1\}$ are the differentially encoded transmitted symbols, i.e.,

$$b_k = b_0 \prod_{i=1}^{k} a_i \tag{2}$$

where $k > 0$ with $a_i \in \{\pm 1\}$ being the information symbols. As an initial reference transmitted symbol, we consider $b_0 = 1$. We assume that the multipath channel is time-invariant within the interval of $Q$ consecutive symbols, and its delay spread is smaller than $T_s$, thus inter symbol interference (ISI) is avoided. Let the channel impulse response (CIR) with $L$ paths, be represented by $g(t) \triangleq \sum_{l=0}^{L-1} \alpha_l \delta(t - \tau_l)$ where $\alpha_l$ and $\tau_l$ are the respective gain and delay of the $l$th path. The received signal $r(t)$ can then be written as

$$\begin{aligned} r(t) &= \sum_{k=0}^{Q} b_k h(t - kT_s) + v(t) \\ &= x(t) + v(t) \end{aligned} \tag{3}$$

where $h(t) \triangleq \sum_{l=0}^{L-1} \alpha_l q(t - \tau_l)$ is the received pulse, and $v(t)$ is the zero-mean additive white Gaussian noise component with variance $\sigma_v^2$. Denoting with $1/T = N/T_s$ the Nyquist sampling rate, the received signal in its Nyquist-rate sampled version can be written as

$$\mathbf{r} \triangleq [\mathbf{r}_0^T, \mathbf{r}_1^T, \cdots, \mathbf{r}_Q^T]^T \tag{4}$$

where

$$\mathbf{r}_k \triangleq [r(kT_s), r(kT_s + T), \cdots, r(kT_s + NT - T)]^T$$

represents the vector of $N$ Nyquist-rate samples corresponding to the $k$th symbol. We can then derive from (3) that

$$\begin{aligned} \mathbf{r}_k &= b_k \mathbf{h} + \mathbf{v}_k \\ &= \mathbf{x}_k + \mathbf{v}_k \end{aligned} \tag{5}$$

where $\mathbf{x}_k = b_k \mathbf{h}$ is the Nyquist-rate version of the signal part of $\mathbf{r}_k$ with

$$\mathbf{h} \triangleq [h(0), h(T), \cdots, h(NT - T)]^T$$

which is assumed to be invariant during the block of $Q$ symbols, and the zero-mean Gaussian distributed Nyquist-rate sampled noise vector is given by

$$\mathbf{v}_k \triangleq [v(kT_s), v(kT_s + T), \cdots, v(kT_s + NT - T)]^T$$

with covariance matrix

$$\mathbf{C}_v \triangleq \mathrm{E}\{\mathbf{v}_k \mathbf{v}_k^T\} = \sigma_v^2 \mathbf{I}_N.$$

## III. MSDD with GLRT

GLRT is a widely used composite hypothesis testing approach where the prior probability density functions (pdfs) of the unknown parameters are not necessarily known. The detection is carried out for each parameter as a likelihood ratio test. Given the absence of channel information, MSDD was proposed in [11] using the GLRT approach. There, the likelihood function is maximized not only over the unknown symbols but also over the channel parameters. Now, from (4) and (5), a joint model of the $Q+1$ symbols can be written as

$$\mathbf{r} = (\mathbf{b} \otimes \mathbf{I}_N)\mathbf{h} + \mathbf{v} \tag{6}$$

where $\mathbf{b} \triangleq [b_0, b_1, \cdots, b_Q]^T$ denotes the transmitted symbols and $\mathbf{v} \triangleq [\mathbf{v}_0^T, \mathbf{v}_1^T, \cdots, \mathbf{v}_Q^T]^T$ is the concatenated noise vector. Defining $\mathbf{a} \triangleq [a_1, a_2, \cdots, a_Q]^T$ as the vector of the actual information symbols, the differential detection of multiple symbols using the GLRT approach boils down to maximizing the following log-likelihood metric over $\mathbf{a}$ and $\mathbf{h}$

$$\begin{aligned} \Lambda[\mathbf{r}|\mathbf{a}, \mathbf{h}] &\triangleq 2\mathbf{r}^T(\mathbf{b} \otimes \mathbf{I}_N)\mathbf{h} - [(\mathbf{b} \otimes \mathbf{I}_N)\mathbf{h}]^T[(\mathbf{b} \otimes \mathbf{I}_N)\mathbf{h}] \\ &= 2\mathbf{r}^T(\mathbf{b} \otimes \mathbf{I}_N)\mathbf{h} - (Q+1)\mathbf{h}^T\mathbf{h} \end{aligned} \tag{7}$$

where $\mathbf{b}$ is a function of $\mathbf{a}$ as described in (2). The detection procedure proceeds in two steps. In step one, (7) is optimized over $\mathbf{h}$, i.e.,

$$\Gamma[\mathbf{r}|\mathbf{a}] \triangleq \max_{\mathbf{h}} \Lambda[\mathbf{r}|\mathbf{a}, \mathbf{h}] \tag{8}$$

and in the second step, (8) is optimized over $\mathbf{a}$, i.e.,

$$\hat{\mathbf{a}} = \arg\max_{\mathbf{a}} \{\Gamma[\mathbf{r}|\mathbf{a}]\}. \tag{9}$$

Thus the Nyquist-rate MSDD (NMSDD) using the GLRT approach solves the following optimization problem

$$\hat{\mathbf{a}}^{(\mathrm{NMSDD})} = \arg\max_{\mathbf{a}} \left\{ \max_{\mathbf{h}} \Lambda[\mathbf{r}|\mathbf{a}, \mathbf{h}] \right\}. \tag{10}$$

## IV. Compressive Sampling based MSDD

For the compressive sampling based MSDD (CMSDD), we consider each received symbol $\mathbf{r}_k$ to be compressed by a measurement process represented by $\mathbf{\Phi}_k$ which is an $M \times N$ wide matrix, i.e., $M \ll N$. The ratio $\mu \triangleq \frac{M}{N}$ is called the compression ratio. In general, we assume that $\mathbf{\Phi}_k \mathbf{\Phi}_k^T = \mathbf{I}_M$. Now, the compressed received signal within one symbol can be expressed as

$$\begin{aligned} \mathbf{y}_k &= \mathbf{\Phi}_k \mathbf{r}_k \\ &= \mathbf{\Phi}_k \mathbf{x}_k + \boldsymbol{\xi}_k \end{aligned} \tag{11}$$

where $\boldsymbol{\xi}_k \triangleq \boldsymbol{\Phi}_k \mathbf{v}_k$ is the noise component with covariance matrix

$$\mathbf{C}_\xi \triangleq \mathrm{E}\{\boldsymbol{\xi}_k \boldsymbol{\xi}_k^T\} = \sigma_v^2 \mathbf{I}_M.$$

It should be noted that the measurement process in (11) is carried out in the analog domain (see, e.g., [14], [15] for details on the analog implementations). Now from (11), we can express the joint model of $Q+1$ compressed symbols as

$$\mathbf{y} = \boldsymbol{\Phi}(\mathbf{b} \otimes \mathbf{I}_N)\mathbf{h} + \boldsymbol{\xi} \tag{12}$$

where $\mathbf{y} = [\mathbf{y}_0^T, \mathbf{y}_1^T \cdots \mathbf{y}_Q^T]^T$ is the $(Q+1)M \times 1$ measurement vector and $\boldsymbol{\Phi} = \mathrm{diag}\{\boldsymbol{\Phi}_0, \boldsymbol{\Phi}_0, \cdots, \boldsymbol{\Phi}_Q\}$ is the $(Q+1)M \times (Q+1)N$ fat measurement matrix with $\boldsymbol{\Phi}\boldsymbol{\Phi}^T = \mathbf{I}_{(Q+1)M}$.

Following the GLRT approach, the MSDD for the compressed symbols requires the maximization of the following log-likelihood metric

$$\begin{aligned}\Lambda[\mathbf{y}|\mathbf{a},\mathbf{h}] &\triangleq 2\mathbf{y}^T\boldsymbol{\Phi}(\mathbf{b}\otimes\mathbf{I}_N)\mathbf{h} \\ &\quad - [(\mathbf{b}\otimes\mathbf{I}_N)\mathbf{h}]^T\boldsymbol{\Phi}^T\boldsymbol{\Phi}[(\mathbf{b}\otimes\mathbf{I}_N)\mathbf{h}] \\ &= 2\mathbf{y}^T\boldsymbol{\Phi}(\mathbf{b}\otimes\mathbf{I}_N)\mathbf{h} - \mathbf{h}^T(\mathbf{b}\otimes\mathbf{I}_N)^T\boldsymbol{\Phi}^T\boldsymbol{\Phi}(\mathbf{b}\otimes\mathbf{I}_N)\mathbf{h} \end{aligned} \tag{13}$$

over $\mathbf{h}$ and $\mathbf{a}$. The CMSDD, basically solves the following optimization problem

$$\hat{\mathbf{a}}^{(\mathrm{CMSDD})} = \arg\max_{\mathbf{a}} \left\{ \max_{\mathbf{h}} \Lambda[\mathbf{y}|\mathbf{a},\mathbf{h}] \right\}. \tag{14}$$

As a first step, we maximize (13) over $\mathbf{h}$. Differentiating (13) with respect to $\mathbf{h}$ and setting the gradient equal to zero yields

$$0 = 2\mathbf{y}^T - 2\mathbf{h}^T(\mathbf{b}\otimes\mathbf{I}_N)^T\boldsymbol{\Phi}^T$$

which leads to the following estimate of $\mathbf{h}$

$$\hat{\mathbf{h}} = [\boldsymbol{\Phi}(\mathbf{b}\otimes\mathbf{I}_N)]^\dagger \mathbf{y}. \tag{15}$$

Now plugging the estimate of $\mathbf{h}$ in (13), we obtain the following cost function

$$\begin{aligned}\Gamma[\mathbf{y}|\mathbf{a}] &\triangleq 2\mathbf{y}^T\boldsymbol{\Phi}(\mathbf{b}\otimes\mathbf{I}_N)\left[\boldsymbol{\Phi}(\mathbf{b}\otimes\mathbf{I}_N)\right]^\dagger\mathbf{y} \\ &\quad - \left[\left[\boldsymbol{\Phi}(\mathbf{b}\otimes\mathbf{I}_N)\right]^\dagger\mathbf{y}\right]^T(\mathbf{b}\otimes\mathbf{I}_N)^T\boldsymbol{\Phi}^T \\ &\quad \times \boldsymbol{\Phi}(\mathbf{b}\otimes\mathbf{I}_N)\left[\boldsymbol{\Phi}(\mathbf{b}\otimes\mathbf{I}_N)\right]^\dagger\mathbf{y}. \end{aligned} \tag{16}$$

The second part of (16) can be defined and simplified as

$$\begin{aligned}\Gamma_2 &\triangleq \left[\left[\boldsymbol{\Phi}(\mathbf{b}\otimes\mathbf{I}_N)\right]^\dagger\mathbf{y}\right]^T(\mathbf{b}\otimes\mathbf{I}_N)^T\boldsymbol{\Phi}^T \\ &\quad \times \boldsymbol{\Phi}(\mathbf{b}\otimes\mathbf{I}_N)\left[\boldsymbol{\Phi}(\mathbf{b}\otimes\mathbf{I}_N)\right]^\dagger\mathbf{y} \\ &= \mathbf{y}^T\left[\left[(\mathbf{b}\otimes\mathbf{I}_N)^T\boldsymbol{\Phi}^T\boldsymbol{\Phi}(\mathbf{b}\otimes\mathbf{I}_N)\right]^{-1}\left[\boldsymbol{\Phi}(\mathbf{b}\otimes\mathbf{I}_N)\right]^T\right]^T \\ &\quad \times (\mathbf{b}\otimes\mathbf{I}_N)^T\boldsymbol{\Phi}^T\boldsymbol{\Phi}(\mathbf{b}\otimes\mathbf{I}_N)\left[\boldsymbol{\Phi}(\mathbf{b}\otimes\mathbf{I}_N)\right]^\dagger\mathbf{y} \\ &= \mathbf{y}^T\boldsymbol{\Phi}(\mathbf{b}\otimes\mathbf{I}_N)\left[(\mathbf{b}\otimes\mathbf{I}_N)^T\boldsymbol{\Phi}^T\boldsymbol{\Phi}(\mathbf{b}\otimes\mathbf{I}_N)\right]^{-1} \\ &\quad \times \left[(\mathbf{b}\otimes\mathbf{I}_N)^T\boldsymbol{\Phi}^T\boldsymbol{\Phi}(\mathbf{b}\otimes\mathbf{I}_N)\right]\left[\boldsymbol{\Phi}(\mathbf{b}\otimes\mathbf{I}_N)\right]^\dagger\mathbf{y} \\ &= \mathbf{y}^T\boldsymbol{\Phi}(\mathbf{b}\otimes\mathbf{I}_N)\left[\boldsymbol{\Phi}(\mathbf{b}\otimes\mathbf{I}_N)\right]^\dagger\mathbf{y}. \end{aligned} \tag{17}$$

Thus (16) can be written as

$$\begin{aligned}\Gamma[\mathbf{y}|\mathbf{a}] &= 2\mathbf{y}^T\boldsymbol{\Phi}(\mathbf{b}\otimes\mathbf{I}_N)\left[\boldsymbol{\Phi}(\mathbf{b}\otimes\mathbf{I}_N)\right]^\dagger\mathbf{y} - \Gamma_2 \\ &= \mathbf{y}^T\boldsymbol{\Phi}(\mathbf{b}\otimes\mathbf{I}_N)\left[(\mathbf{b}\otimes\mathbf{I}_N)^T\boldsymbol{\Phi}^T\boldsymbol{\Phi}(\mathbf{b}\otimes\mathbf{I}_N)\right]^{-1} \\ &\quad \times (\mathbf{b}\otimes\mathbf{I}_N)^T\boldsymbol{\Phi}^T\mathbf{y} \\ &= \mathbf{y}^T\boldsymbol{\Phi}(\mathbf{b}\otimes\mathbf{I}_N)\boldsymbol{\Sigma}^{-1}(\mathbf{b}\otimes\mathbf{I}_N)^T\boldsymbol{\Phi}^T\mathbf{y} \end{aligned} \tag{18}$$

where

$$\begin{aligned}\boldsymbol{\Sigma} &\triangleq \left[(\mathbf{b}\otimes\mathbf{I}_N)^T\boldsymbol{\Phi}^T\boldsymbol{\Phi}(\mathbf{b}\otimes\mathbf{I}_N)\right] \\ &= \left[b_0^2\boldsymbol{\Phi}_0^T\boldsymbol{\Phi}_0 + b_1^2\boldsymbol{\Phi}_1^T\boldsymbol{\Phi}_1 + \cdots + b_Q^2\boldsymbol{\Phi}_Q^T\boldsymbol{\Phi}_Q\right] \\ &= \left[\boldsymbol{\Phi}_0^T\boldsymbol{\Phi}_0 + \boldsymbol{\Phi}_1^T\boldsymbol{\Phi}_1 + \cdots + \boldsymbol{\Phi}_Q^T\boldsymbol{\Phi}_Q\right] \end{aligned} \tag{19}$$

We can see that $\boldsymbol{\Sigma}$ is a positive (semi-)definite matrix. As has been explained at length in [18] for (18)-like scenarios, assuming that $\boldsymbol{\Sigma}^{-1}$ does not affect the differential estimate of the vectors on its sides, the maximum of (18) will be the maximum of

$$\begin{aligned}\tilde{\Gamma}[\mathbf{y}|\mathbf{a}] &\triangleq \mathbf{y}^T\boldsymbol{\Phi}(\mathbf{b}\otimes\mathbf{I}_N)(\mathbf{b}\otimes\mathbf{I}_N)^T\boldsymbol{\Phi}^T\mathbf{y} \\ &= \mathbf{y}^T\boldsymbol{\Phi}(\mathbf{b}\mathbf{b}^T\otimes\mathbf{I}_N)\boldsymbol{\Phi}^T\mathbf{y} \end{aligned} \tag{20}$$

and the CMSDD then boils down to

$$\hat{\mathbf{a}} = \arg\max_{\mathbf{a}} \left\{ \tilde{\Gamma}[\mathbf{y}|\mathbf{a}] \right\}. \tag{21}$$

The structure of the cost function (20) contains the different possible differential combinations of $Q+1$ symbols, i.e.,

$$\begin{aligned}\tilde{\Gamma}[\mathbf{y}|\mathbf{a}] &= \mathbf{y}^T\boldsymbol{\Phi}(\mathbf{b}\mathbf{b}^T\otimes\mathbf{I}_N)\boldsymbol{\Phi}^T\mathbf{y} \\ &= b_0b_0\mathbf{y}_0^T\boldsymbol{\Phi}_0\boldsymbol{\Phi}_0^T\mathbf{y}_0 + \cdots + b_0b_Q\mathbf{y}_0^T\boldsymbol{\Phi}_0\boldsymbol{\Phi}_Q^T\mathbf{y}_Q \\ &\quad + b_1b_0\mathbf{y}_1^T\boldsymbol{\Phi}_1\boldsymbol{\Phi}_0^T\mathbf{y}_0 + \cdots + b_1b_Q\mathbf{y}_1^T\boldsymbol{\Phi}_1\boldsymbol{\Phi}_Q^T\mathbf{y}_Q \\ &\quad + \cdots + \\ &\quad + b_Qb_0\mathbf{y}_Q^T\boldsymbol{\Phi}_Q\boldsymbol{\Phi}_0^T\mathbf{y}_0 + \cdots + b_Qb_Q\mathbf{y}_Q^T\boldsymbol{\Phi}_Q\boldsymbol{\Phi}_Q^T\mathbf{y}_Q \end{aligned} \tag{22}$$

which reveals a number of interesting points.

1) If the measurement matrices are orthogonal to each other for all symbols, i.e.,

$$\boldsymbol{\Phi}_0 \perp \boldsymbol{\Phi}_1 \perp \cdots \perp \boldsymbol{\Phi}_Q$$

then the detector does not exist.

2) If the measurement matrices are the same for each symbol, i.e.,

$$\boldsymbol{\Phi}_0 = \boldsymbol{\Phi}_1 = \cdots = \boldsymbol{\Phi}_Q$$

then the detector can be derived by solving the following cost function

$$\tilde{\Gamma}[\mathbf{y}|\mathbf{a}] = \sum_{k=1}^{Q}\sum_{l=0}^{k-1}\prod_{i=1}^{k-l}[\mathbf{a}]_{i+l}\mathbf{y}_l^T\mathbf{y}_k \tag{23}$$

3) In case the measurement matrices are not orthogonal and not the same, the cost function is

$$\tilde{\Gamma}[\mathbf{y}|\mathbf{a}] = \sum_{k=1}^{Q}\sum_{l=0}^{k-1}\prod_{i=1}^{k-l}[\mathbf{a}]_{i+l}\mathbf{y}_l^T\boldsymbol{\Phi}_l\boldsymbol{\Phi}_k^T\mathbf{y}_k \tag{24}$$

Items 1 and 2 above, provide performance limits for our compressed differential detector. Better performance is achieved if the measurement process is the same for each symbol. If the measurement matrices are orthogonal to each other, then the compressed detector cannot perform. In applications where maintaining an identical measurement process for each received symbol is not feasible, given that the orthogonality of the process has been avoided, (24) can still offer compressed detection.

## V. Compressed Sphere Decoder

It can be seen from (23) and (24), that maximizing these cost functions over $\mathbf{a}$ involves an exhaustive search over all the possible combinations of the vector $\mathbf{a}$ along with first intercorrelating all symbols in the block of symbols. Since correlations are carried out in the digital domain and more so, directly on the compressed symbols without reconstruction, we have already avoided the problem of analog delay lines plus reconstruction complexities. What remains is to reduce or limit the search space over the different possible combinations of $\mathbf{a}$ to find the block of transmitted information symbols. To this end we turn to sphere decoding (SD), which was proposed for the MSDD in [9] for Rayleigh fading channels. SD was applied to the GLRT based MSDD in [11]. In our case, the SD algorithm shall work on the compressed symbols. We shall refer to it as the compressed sphere decoder (CSD).

In SD, the lattice points (e.g., $\mathbf{s}$) are assumed to have the finite alphabet constraint. Then in an iterative fashion, only those points $\mathbf{s}$ are considered which lie inside a sphere of radius $\rho$. Given that $\mathbf{U}$ is an upper triangular matrix, the sphere condition can be written as $\|\mathbf{U}\mathbf{s}\|_2^2 \leq \rho$. During successive iterations, the radius of the sphere keeps decreasing and thus the search space keeps shrinking which results in reduced computational complexity. To make our cost function SD-compatible, we will have to reformulate (24) in a different form. Since the maximum value of our cost function can be written as

$$\tilde{\Gamma}_{max}[\mathbf{y}|\mathbf{a}] \triangleq \sum_{k=1}^{Q}\sum_{l=0}^{k-1} |Y_{l,k}| \tag{25}$$

where $Y_{l,k} \triangleq \mathbf{y}_l^T \mathbf{\Phi}_l \mathbf{\Phi}_k^T \mathbf{y}_k$, the new cost function, after subtracting (24) from (25), can be written as

$$\Theta[\mathbf{y}|\mathbf{a}] \triangleq \sum_{k=1}^{Q}\sum_{l=0}^{k-1} \left[ |Y_{l,k}| - Y_{l,k} \prod_{i=1}^{k-l} [\mathbf{a}]_{i+l} \right] \tag{26}$$

where, depending upon $\prod_{i=1}^{k-l}[\mathbf{a}]_{i+l}$, each addend of (26) will take a value in $\{0, 2\,|Y_{l,k}|\}$. Now the compressed MSDD detector (21) can be written as

$$\hat{\mathbf{a}} = \arg\max_{\mathbf{a}} \{\Theta[\mathbf{y}|\mathbf{a}]\}. \tag{27}$$

At the $n$th iteration, for any tentative $\hat{\mathbf{a}}(n)$ to lie within a sphere of radius $\rho(n)$, the following condition must hold

$$\theta_j \triangleq \sum_{k=1}^{j}\sum_{l=0}^{k-1} \left[ |Y_{l,k}| - Y_{l,k} \prod_{i=1}^{k-l} [\hat{\mathbf{a}}(n)]_{i+l} \right] \leq \rho(n) \tag{28}$$

where $j = 1, \cdots, Q$. At the onset of the algorithm, $\rho(0)$ is chosen large enough so that the optimal value of $\mathbf{a}$ lies within the sphere. Also, it is clear from (28) that at every iteration, already estimated elements of $\hat{\mathbf{a}}$ can be directly used in estimating the next element. So within each iteration, CSD checks $Q$ conditions in a sequential manner. At the end of an iteration, the estimated $\hat{\mathbf{a}}$ is assumed to be the optimal estimate. The next iteration then begins by decreasing the sphere radius, i.e., $\rho(n+1) < \rho(n)$. At a given iteration, if no estimate can be found within the sphere then the CSD terminates and the estimate of the previous iteration is retained as the resultant optimal estimate. The search process can be further simplified by pre-computing the correlation values between the symbols and furthermore by substituting $|Y_{l,k}| = 1$ and retaining only the sign of the correlation value in (28).

## VI. Simulation Results

In this section we gage the performance of our CMSDD with the help of Monte Carlo simulations. The transmitted signal consists of differentially encoded symbols. The transmitted pulses are unit energy pulses (second derivative of a Gaussian function) with width $T_q = 1$nsec. The receive filter bandwidth is taken to be 2GHz. Assuming a frame length (in our case that is also the symbol length since we consider each symbol to consist of a single frame for the sake of simplicity) of $T_s = 50$nsec, each symbol consists of $N = 200$ Nyquist-rate samples. The signal travels through a slow fading channel, modeled by the IEEE 802.15.3a CM1 channel model. The maximum channel delay spread is restricted to 25nsec which means that the received symbol frame without noise has an order of sparsity equal to half of the symbol length. The transmitted signal is detected in a block of $Q = 1, 10, 19$ symbols for which the channel is assumed to be invariant.

For the compressed symbols, we assume a compression ratio of $\mu = 0.5$, i.e., $M = 100$ compressed samples. So we are sampling at half the Nyquist rate. We consider a random Gaussian measurement matrix whose rows have been orthonormalized. We consider two scenarios for these measurement matrices. In scenario one, each symbol is compressed using the same measurement matrix, as expressed under item 2. In scenario two, each received symbol is compressed using a different measurement matrix, as pointed out in item 3.

Figures 1 and 2 show the bit error rate (BER) performance of the CMSDD detector against the $E_b/N_0$ ratio defined as

$$\frac{E_b}{N_0} \triangleq \frac{\|\mathbf{h}\|_2^2}{\sigma_v^2}$$

for the two aforementioned scenarios regarding the measurement matrices. From Figure 1 we can see that the gap between the performance results of the Nyquist-rate MSDD and the compressed-rate MSDD is at most around 2dB at a BER of $10^{-3}$ for all block sizes. When $Q = 1$, the MSDD reduces to the classical DD which results in the worst performance but with increasing block sizes, the performance gets better for both the Nyquist-rate and the compressed-rate detectors. However, the CMSDD has an edge over the Nyquist rate in

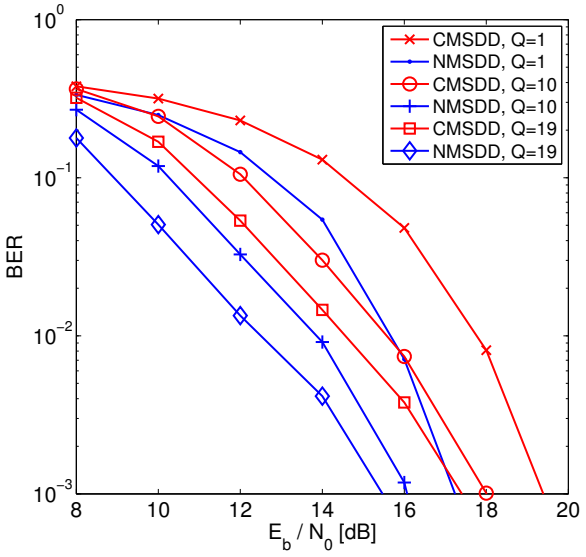


Fig. 1. BER comparison between NMSDD and CMSDD for different block sizes with $\mathbf{\Phi}_k = \mathbf{\Phi}_{k+1}$ and compression ratio $\mu = 0.5$.

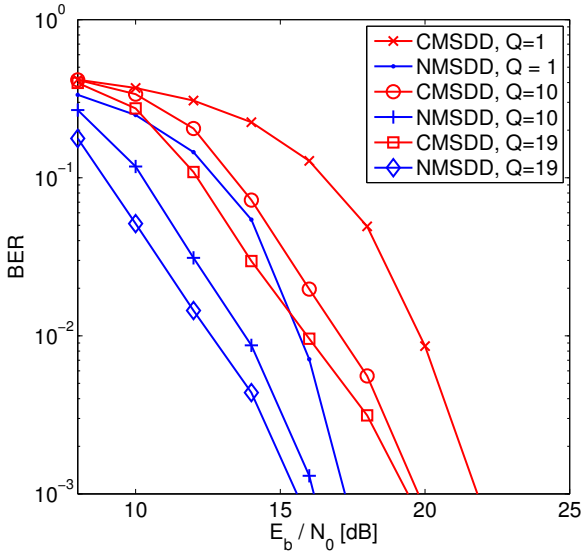


Fig. 2. BER comparison between NMSDD and CMSDD for different block sizes with $\mathbf{\Phi}_k \neq \mathbf{\Phi}_{k+1}$ and compression ratio $\mu = 0.5$.

terms of reducing the sampling rate and in terms of detecting the symbols using compressed samples. Figure 2 shows that the performance gap for the CMSDD for different measurement matrices increases to around 3dB if the measurement matrices are not the same, which is higher than in the former scenario. Thus, different measurement matrices for different symbols result in a performance loss. A logical inference of this observation would mean a worst performance of the detector in case the measurement matrices are orthogonal to each other. This has already been observed under item 1.

## VII. Conclusions

In this paper we have presented a compressive sampling based MSDD using the GLRT approach. The detector avoids the explicit reconstruction step and operates on the compressed samples directly. The detector performs better when the measurement matrices are the same for each symbol within the block but has the ability to work even when they are different. The detector does not exist for the case of orthogonal measurement matrices. Combined with sphere decoding, the proposed detector offers a low complexity and power efficient detection possibilities.

## References


[1] M. Z. Win and R. A. Scholtz, "Impulse radio: how it works," *IEEE Communications Letters*, vol. 2, no. 2, pp. 36–38, Feb. 1998.

[2] M. Ghavami, L. B. Michael and R. Kohno, *Ultra Wideband: signals and systems in communication engineering*, 2nd ed. West Sussex, England: John Wiley and Sons, 2007.

[3] A. F. Molisch, J. R. Foerster and M. Pendergrass, "Channel models for ultrawideband personal area networks", *IEEE Wireless Communications*, vol. 10, no. 6, pp. 14–21, Dec. 2003.

[4] J. D. Choi and W. E. Stark, "Performance of ultra-wideband communications with suboptimal receivers in multipath channels," *IEEE J. Select. Areas Commun.*, vol. 20, no. 9, pp. 1754–1766, Dec. 2002.

[5] V. Lottici, A. N. D'Andrea and U. Mengali, "Channel Estimation for Ultra-Wideband Communications," *IEEE JSAC*, vol. 20, pp. 1638–1645, Dec. 2002.

[6] K. Witrisal, G. Leus, G. Janssen, M. Pausini, F. Troesch, T. Zasowski, and J. Romme, "Noncoherent ultra-wideband systems," *IEEE Signal Processing Magazine*, vol. 26, no. 4, pp. 48–66, July 2009.

[7] R. Hoctor and H. Tomlinson, "Delay-hopped transmitted-reference RF communications,", *Proc. IEEE UWBST2002*, pp. 265–269, 2002.

[8] M. Ho, S. Somayazulu, J. Foerster, S. Roy, "A differential detector for UWB communications system," *IEEE VTC2002*, vol. 4, pp. 1896–1900, May 2002.

[9] L. Lampe, R. Schober, V. Pauli and C. Windpassinger, "Multiple-symbol differential sphere decoding," *IEEE Transaction on Wireless Communications*, vol. 53, no. 12, pp. 1981–1985, Dec. 2005.

[10] N. Guo and R. C. Qiu, "Improved autocorrelation demodulation receivers based on multiple–symbol detection for uwb communications," *IEEE Tran. on Wireless Commun.*, vol. 5, no. 8, Aug. 2006.

[11] V. Lottici, Z. Tian, "Multiple symbol differential detection for UWB communications," *IEEE Trans. Wireless Commun.*, vol. 7, no. 5, pp. 1656–1666, 2008.

[12] D. L. Donoho, "Compressed sensing," *IEEE Transactions on Information Theory*, vol. 52, no. 4,April 2006.

[13] E. Candès, J. Romberg and T. Tao, "Robust uncertainty principles: exact signal reconstruction from highly incomplete frequency information," *IEEE Transaction on Information Theory*, vol. 52, no. 2, pp. 489–509, February 2006.

[14] S. Kirolos, J. Laska, M. Wakin, M. Duarte, D. Baron, T. Ragheb, Y. Massoud, R. Baraniuk, "Analog-to-information conversion via random demodulation," *Proc. IEEE Dallas Circuits and Systems Workshop* (DCAS), 2006.

[15] T. Ragheb, J. Laska, H. Nejati, S. Kirolos, R. Baraniuk, and Y. Massoud, "A prototype hardware for random demodulation based compressive analog-to-digital conversion," *Proc. MWSCAS 2008*, pp. 37–40, Aug. 2008.

[16] A. Oka and L. Lampe, "A compressed sensing receiver for uwb impulse radio in bursty applications like wireless sensor networks," *Physical Communication*, vol. 2, no. 4, pp. 248–264, Dec. 2009.

[17] Z. Wang, G. R. Arce, J. L. Paredes and B. M. Sadler, "Compressed detection for ultra-wideband impulse radio," *IEEE SPAWC*, 2007.

[18] S. Gishkori, G. Leus and V. Lottici, "Compressive sampling based differential detection for uwb impulse radio signals," *Elsevier Physical Communication*, vol. 5, issue 2, June 2012.

[19] A. Schenk and R. F. H. Fischer, "Compressed-sensing (decision-feedback) differential detection in impulse-radio ultra-wideband systems," *Proc. ICUWB*, 2011.

[20] S. M. Kay, *Fundamentals of Statistical signal processing, Detection theory*, Prentice Hall, New Jersey, 1998.